Human differentiated adipocytes can serve as surrogate mature adipocytes for adipocyte-derived extracellular vesicle analysis.

Bradley L. Butsch[1#], Mangesh Dattu Hade[1#], Paola Loreto Palacio[1], Kim Truc Nguyen[2], Dharti Shantaram[3], Sabrena Noria[4], Stacy A. Brethauer[4], Bradley J. Needleman[4], Willa Hsueh[3], Eduardo Reátegui[2], Setty M. Magaña[1*]

[1]Department of Pediatrics, Center for Clinical and Translational Research, Nationwide Children's Hospital, Columbus, Ohio.

[2]Department of Chemical and Biomedical Engineering, The Ohio State University, Columbus, Ohio.

[3]Diabetes and Metabolism Research Center, The Ohio State University, Columbus, Ohio.

[4]Center for Minimally Invasive Surgery, Department of Surgery, The Ohio State University College of Medicine, Columbus, Ohio.

# Authors contributed equally.

Running Title: Human differentiated adipocyte extracellular vesicles

***Corresponding Author:** Setty Magaña, MD, PhD

Address: Nationwide Children's Hospital
Department of Pediatrics, Division of Neurology
700 Children's Drive
Columbus, OH 43205

Telephone: 614-722-4625

Fax: 614-722-4633

Email: Setty.Magana@nationwidechildrens.org

Abstract

Obesity is a growing global health concern, contributing to diseases such as cancer, autoimmune disorders, and neurodegenerative conditions. Adipose tissue dysfunction, characterized by abnormal adipokine secretion and chronic inflammation, plays a key role in these conditions. Adipose-derived extracellular vesicles (ADEVs) have emerged as critical mediators in obesity-related diseases. However, the study of mature adipocyte-derived EVs (mAdipo-EVs) is limited due to the short lifespan of mature adipocytes in culture, low EV yields, and the low abundance of these EV subpopulations in the circulation. Additionally, most studies rely on rodent models, which have differences in adipose tissue biology compared to humans. To overcome these challenges, we developed a standardized approach for differentiating human preadipocytes (preAdipos) into mature differentiated adipocytes (difAdipos), which produce high-yield, human adipocyte EVs (Adipo-EVs). Using visceral adipose tissue from bariatric surgical patients, we isolated the stromal vascular fraction (SVF) and differentiated preAdipos into difAdipos. Brightfield microscopy revealed that difAdipos exhibited morphological characteristics comparable to mature adipocytes (mAdipos) directly isolated from visceral adipose tissue, confirming their structural similarity. Additionally, qPCR analysis demonstrated decreased preadipocyte markers and increased mature adipocyte markers, further validating successful differentiation. Functionally, difAdipos exhibited lipolytic activity comparable to mAdipos, supporting their functional resemblance to native adipocytes. We then isolated preAdipo-EVs and difAdipo-EVs using tangential flow filtration and characterized them using bulk and single EV analysis. DifAdipo-EVs displayed classical EV and adipocyte-specific markers, with significant differences in biomarker expression compared to preAdipo-EVs. These findings demonstrate that difAdipos serve as a reliable surrogate for mature adipocytes, offering a consistent and scalable source of adipocyte-derived EVs for studying obesity and its associated disorders.

Keywords: extracellular vesicles, adipocyte, adipose, adipocyte-derived extracellular vesicles, obesity

Introduction

The widespread prevalence of obesity has escalated into a formidable global health emergency, placing significant burdens on public health systems worldwide [1,2]. In 2019, an estimated 5 million obesity-related deaths occurred worldwide [3]. Obesity is intricately linked to various metabolic disorders, including type 2 diabetes mellitus, cardiovascular diseases and non-alcoholic fatty liver disease [4-6]. Moreover, obesity is also implicated in the pathogenesis of several cancers, autoimmune diseases, and neurodegenerative disorders [7,8]. The complex interplay between obesity and these diseases underscores the multifaceted role of adipose tissue in maintaining metabolic homeostasis and overall health [9,10]. Adipose tissue, a dynamic endocrine organ, significantly influences energy balance, metabolic regulation, and immune responses [11]. Dysfunctional adipose tissue, characterized by altered adipokine secretion, chronic inflammation, and impaired adipocyte differentiation, is a hallmark of obesity and a crucial factor in the emergence of obesity-related comorbidities [12,13]. Recent research advances have illuminated the pivotal role of extracellular vesicles (EVs) in mediating intercellular communication and regulating metabolic processes [14,15]. EVs are small, membrane-bound particles secreted by cells that transport bioactive molecules (e.g. proteins, lipids, and nucleic acids) to recipient cells, thereby altering recipient cell genotypic and phenotypic function [14-16].

Mounting evidence indicates that obesity is associated with enhanced production of adipose-derived EVs (ADEVs), which are instrumental in the pathogenesis of obesity and its related metabolic complications [17-19]. ADEVs are implicated in various physiological and pathological processes, including inflammation, insulin resistance, and lipid metabolism [19,20].

Despite the growing interest in studying ADEVs, there is a dearth of human ADEV studies, partly due to the technical and biological limitations of obtaining EVs from mature human adipocytes (mAdipo-EVs). mAdipos exhibit short viability in culture, produce low yields of EVs, and are difficult to handle due to their nonadherent properties [21-23]. To address these limitations, and with the end goal of developing a

robust human translational paradigm for isolating mature adipocyte-derived EVs, we first developed a surrogate mAdipo model by differentiating human preAdipos into mature-like difAdipos with functional, genotypical, and phenotypical similarities to mature adipocytes. Secondly, we used the validated difApos as a reliable and surrogate source of human adipocyte EVs, demonstrating classic EV and adipose markers.

In summary, our study provides a reproducible and reliable source of human mature-like adipose EVs. By leveraging human-based models, we aim to provide a more relevant understanding of the role of adipocyte-derived EVs in obesity-related disorders, thus addressing the critical need for human-based obesity EV paradigms [24].

Results

Multiparametric isolation and characterization of ADEVs

We have developed a comprehensive pipeline for isolating and characterizing EVs from various human adipose tissue biospecimens (**Figure 1, Table S2)**[25]. While most human EV biomarker studies have focused on biofluids or in vitro EV sources, isolating tissue-derived EVs presents technical challenges that must be addressed to maintain the integrity of both the cells and the EVs[29]. To ensure our isolation method produced intact adipocyte-derived EVs, we performed extensive bulk and single EV characterization, as detailed below in **Figure 1.**

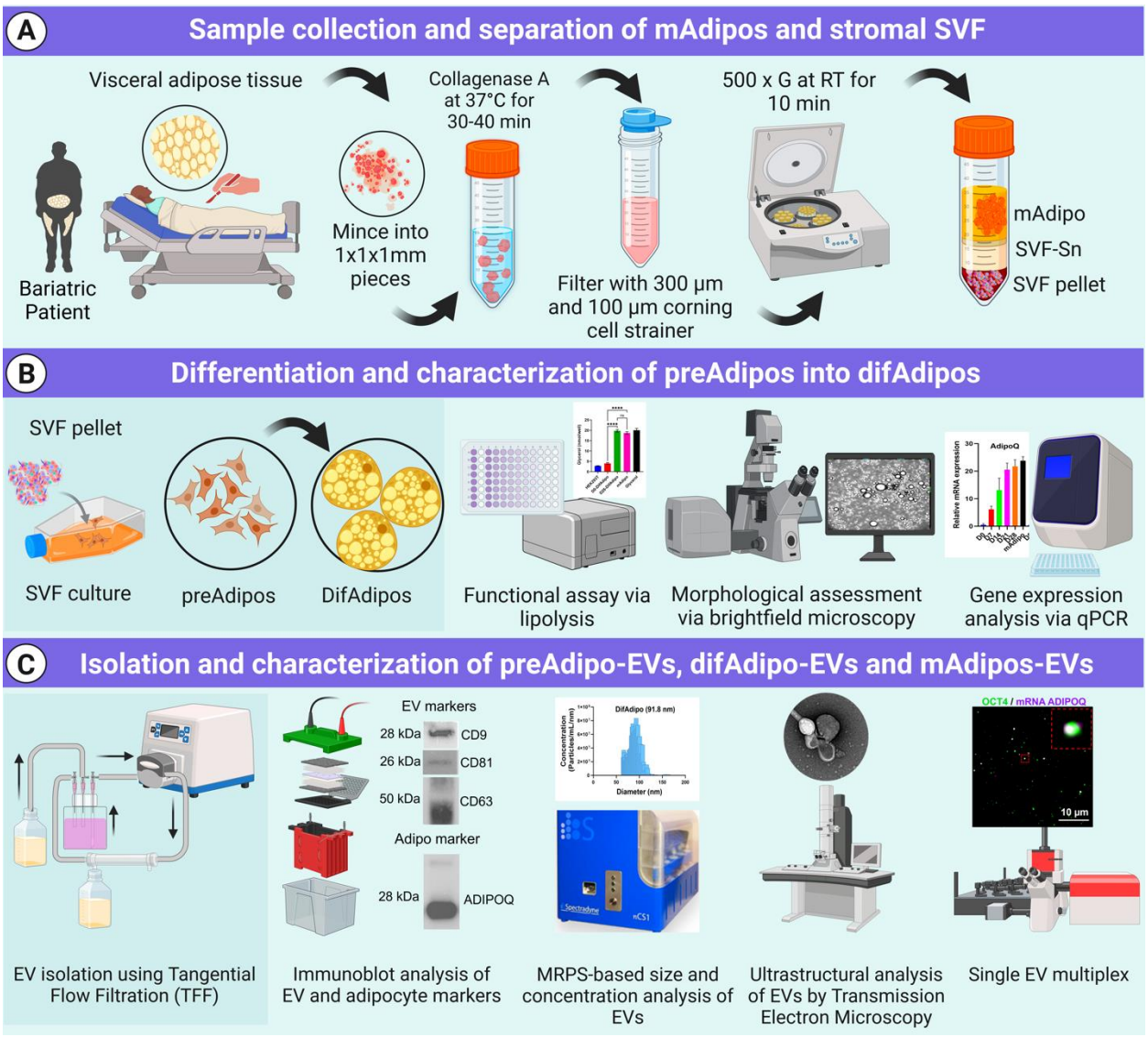

Figure 1. Workflow for the isolation, differentiation, and characterization of human preadipocytes, differentiated adipocytes, and their EVs. (A): Visceral adipose tissue obtained from bariatric patients was enzymatically digested using Collagenase A at 37°C for 30–40 minutes, followed by filtration through 300 µm and 100 µm cell strainers. Subsequent centrifugation (500 × g, RT, 10 min) yielded three distinct fractions: stromal vascular fraction (SVF), SVF supernatant (SVF-SN), and mature adipocytes (mAdipos). The SVF-derived preadipocytes (preAdipos) were cultured and induced to differentiate into differentiated mature adipocytes (difAdipos) over 28 days. Conditioned media from adipocyte cultures were collected and processed using tangential flow filtration (TFF) for EV isolation. (B): Characterization of preAdipos, difAdipos and mAdipos included

95 functional assays assessing lipolysis, morphological analysis via brightfield microscopy,
96 and gene expression analysis using quantitative PCR. (C): Isolated EVs from preAdipos
97 (preAdipo-EVs) and difAdipos (difAdipo-EVs) underwent extensive characterization,
98 including immunoblot analysis of EV and adipocyte markers (CD9, CD81, CD63, and
99 ADIPOQ), size distribution and concentration analysis via microfluidic resistive pulse
100 sensing (MRPS), ultrastructural evaluation using transmission electron microscopy
101 (TEM), and single-EV multiplexing analysis. extracellular vesicles (EVs); stromal
102 vascular fraction (SVF), SVF supernatant (SVF-SN), mature adipocytes (mAdipos);
103 preadipocytes (preAdipos); differentiated mature adipocytes (difAdipos); microfluidic
104 resistive pulse sensing (MRPS); transmission electron microscopy (TEM)
105
106 **Visceral adipose-derived preadipocytes serve as a surrogate source for mature**
107 **adipocytes**
108 Our robust and systematic human-based protocol for isolating, differentiating, and
109 characterizing SVF-derived preadipocytes yielded a reliable surrogate source of
110 differentiated mature adipocytes (difAdipos) (see material and methods). Preadipocytes
111 exhibited significant morphological changes during the differentiation process,
112 accumulating larger lipid droplets and developing a mature phenotype, as confirmed by
113 brightfield imaging (Figure 2B).

114

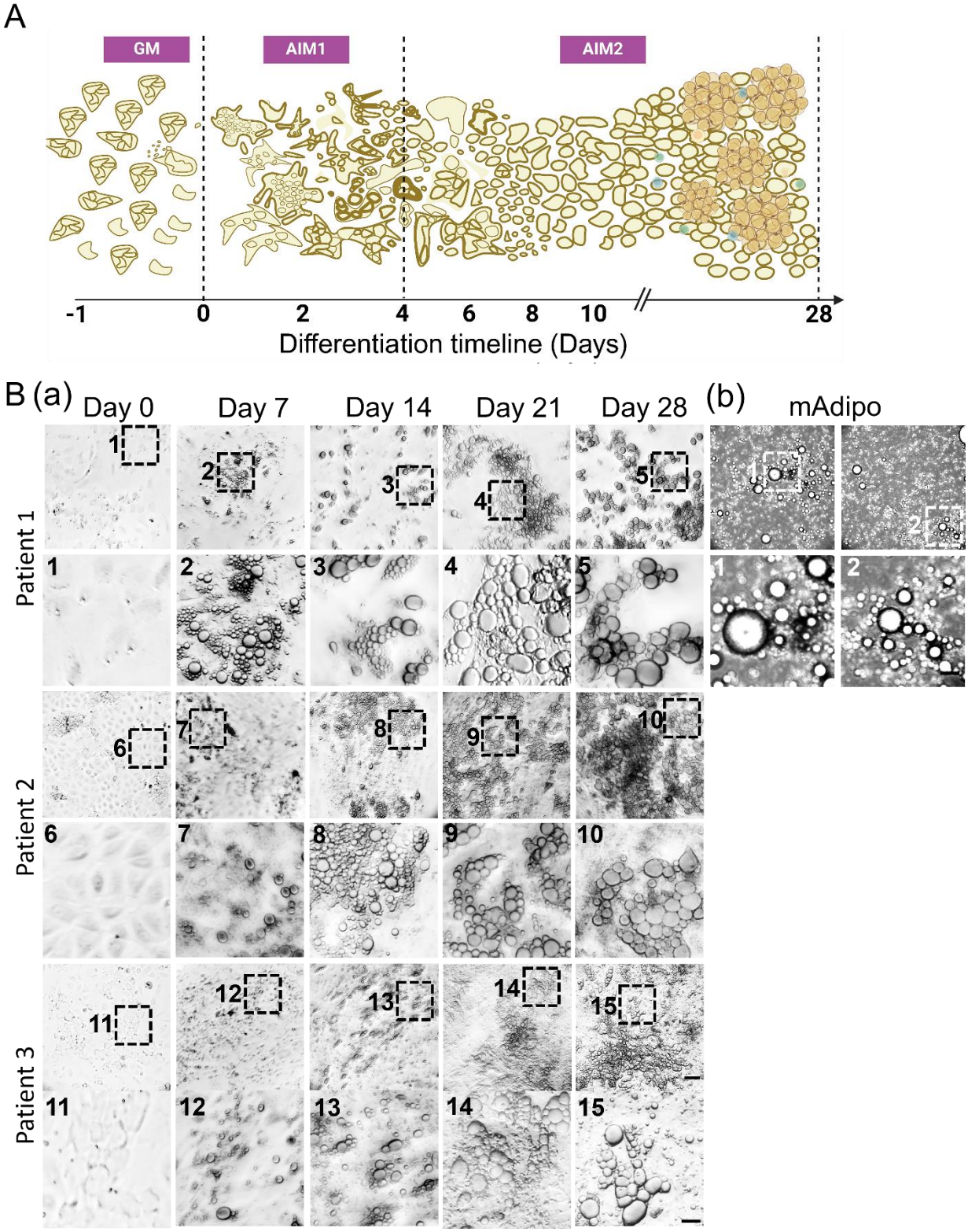
A
GM
AIM1
AIM2
-1
0
2
4
6
8
10
28
Differentiation timeline (Days)
B (a)
Day 0
Day 7
Day 14
Day 21
Day 28
(b)
mAdipo
Patient 1
Patient 2
Patient 3

115

116 **Figure 2. Human preadipocytes undergo differentiation and acquire a mature**
117 **adipocyte phenotype.** (A) Differentiation timeline: At Day -1, cells reached ~80%
118 confluency in growth medium (GM). Differentiation was initiated on Day 0 following a 24-
119 hour incubation in GM by replacing the medium with adipogenic induction medium 1
120 (AIM1). The transition to adipogenic induction medium 2 (AIM2) was performed to
121 facilitate further maturation, leading to the acquisition of a differentiated mature
122 adipocyte (difAdipo) phenotype by Day 28. (B) Morphological changes during
123 adipogenesis: (a) Representative brightfield microscopy images illustrate the
124 progressive morphological changes occurring during preadipocyte differentiation into
125 difAdipos. Lipid droplet accumulation becomes progressively evident throughout the
126 differentiation process. (b) The morphology of difAdipos at Day 28 closely resembles
127 that of primary mature adipocytes (mAdipos), which were directly isolated from patient-
128 derived visceral adipose tissue and maintained in culture for 24 hours.
129 Images are representative of three independent biological replicates (n = 3). Dashed
130 boxes highlight selected regions, which are shown as enlarged high-magnification
131 images in the subsequent panels to provide detailed visualization of cellular
132 morphology. Scale bar = 50 μm for main images; 10 μm for enlarged high-magnification
133 images. GM, growth medium; AIM1, adipogenic induction medium 1; AIM2, adipogenic
134 induction medium 2. differentiated mature adipocyte (difAdipo); mature adipocytes
135 (mAdipos)
136
137 **Differential expression of preadipocyte and mature adipocyte markers during**
138 **adipocyte differentiation**
139 We next investigated gene transcripts of known preAdipo markers (OCT4, PREF-
140 1, and GATA3) [30-33] [30] and mature adipocyte markers (ADIPOQ, PLIN1, and PPARG) [34]
141 at different time points during adipocyte differentiation (**Figure 3**). We hypothesized that
142 difAdipos would acquire a genetic program similar to mAdipos and lose the
143 undifferentiated transcript profile that characterizes preAdipos. As expected [35,36], OCT4
144 expression was low at Day 0 (D0), peaked at D7 ($P < 0.001$), and decreased as
145 differentiation progressed and cells committed adipogenesis (**Figure 3A**).

We saw a similar pattern in PREF-1 expression levels. PREF-1 is an inhibitor of adipogenesis and it is downregulated as cells undergo differentiation [36]. Consistent with this observation, preAdipo PREF-1 levels were relatively low at D0, peaked at D7($P < 0.0001$), and were decreased by D28 and in mAdipos (**Figure 3A**). In contrast to OCT4 and PREF-1, GATA3 levels persisted in both the early and intermediate differentiation stages. GATA3 expression peaked at D7 ($P < 0.01$) and D14, decreased through D21 and D28, but remained elevated in mAdipo compared to D28 (**Figure 3A**). This expression pattern is consistent with studies showing GATA3's involvement in regulating adipogenesis [37,38].

Concurrently, the expression of the mature adipocyte markers ADIPOQ, PLIN1, and PPARG, showed a clear increasing trend during differentiation, as previously reported [38-40]. ADIPOQ expression was low at D0 and D7, increased steadily from D14 onwards, and peaked at D28 ($P < 0.0001$), with levels comparable to those seen in our mAdipos (**Figure 3B**). PLIN1 plays a crucial role in regulating lipid storage and mobilization by protecting lipid droplets from lipolysis in adipocytes [41]. We observed gradually increasing levels of PLIN1 expression from D0 onward, significantly increasing at D21 and D28 ($P < 0.0001$), signifying lipid accumulation and adipocyte maturation. Similarly, PPARG expression progressively increased from D0 to D28, with the highest expression observed at D21 and D28 ($P < 0.0001$), and slightly lower expression in mAdipo, highlighting its crucial role as a regulator of adipogenesis (**Figure 3B**). In summary, the dynamic transcriptional program we observed reflects the successful differentiation of preadipocytes into difAdipos exhibiting mature adipocyte transcriptional profiles.

177 **A**

178

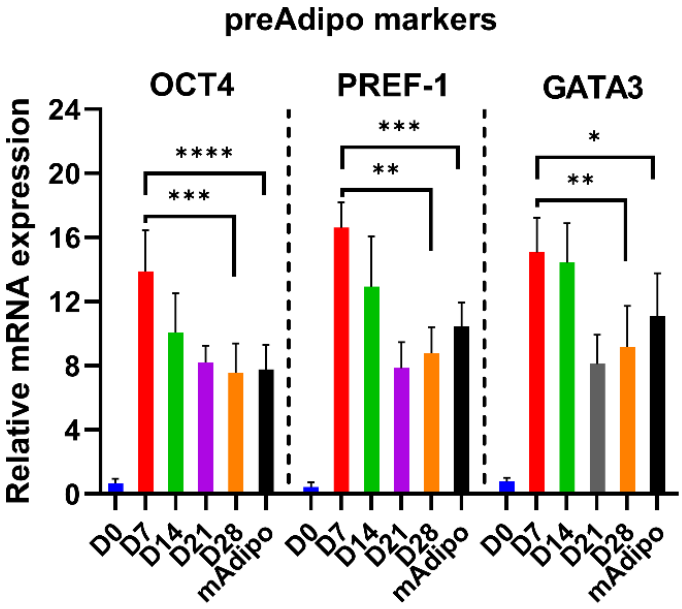

179

180 **B**

181

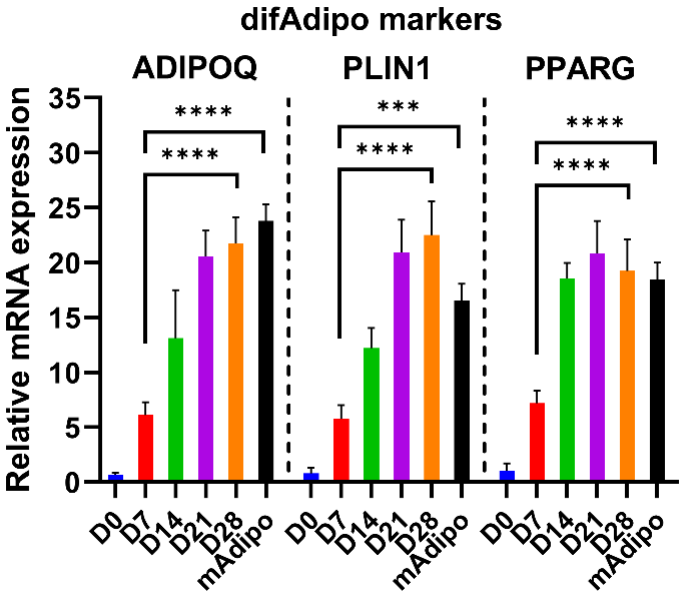

182

183 **Figure 3. Transcript profile in preadipocytes, differentiated adipocytes and**

184 **mature adipocyte (A)** Relative mRNA expression levels of preadipocyte markers

185 (OCT4, PREF1, GATA3) and **(B)** mature adipocyte markers (ADIPOQ, PLIN1, PPARG)

were measured at Day 0 (D0), D7, D14, D21, D28, and in terminally differentiated mAdipo. OCT4 expression peaked at D7 and decreased thereafter, indicating early differentiation. PREF-1 expression increased to a peak at D7 and decreased towards D28, consistent with its inhibitory role in adipogenesis. GATA3 expression peaked at D7 and D14 and remained elevated in mAdipo, indicating its involvement in early differentiation. Adipocyte markers ADIPOQ, PLIN1, and PPARG exhibited a progressive increase, peaking at D28 and in mAdipo, reflecting mature adipocyte function (n=3). The statistical analysis was performed using ordinary one-way ANOVA with Bartlett's test. OCT4, octamer-binding transcription factor 4; PREF-1, preadipocyte factor 1; GATA3, GATA-binding protein 3; ADIPOQ, adiponectin; PLIN, perilipin; PPARG, peroxisome proliferator-activated receptor gamma. A value of $P < 0.05$ was deemed statistically significant (*< 0.05; **< 0.01; ***< 0.001; ****< 0.0001).

Differentiated adipocytes exhibit lipolytic function comparable to mature adipocytes

Preadipocytes differentiated in vitro may not retain the same biophysical properties of mature adipocytes that are differentiated in vivo[42]. Therefore, we next sought to functionally validate the mAdipo phenotype of our difAdipos by investigating their ability to perform the prototypic mature adipocyte function of lipolysis [43-45]. Cells were stimulated with the lipolytic agent, isoproterenol, and lipolysis was assessed by quantifying the stimulated release of glycerol into the culture medium (**Figure 4**). We hypothesized that the lipolytic activity of difAdipos would not differ from that of mAdipos, suggesting that our difAdipos could serve as functional surrogates of mAdipos. Compared to undifferentiated D0 preadipocytes, D28 difAdipos achieved a comparable degree of lipolytic activity as mAdipos. These findings demonstrate our ability to generate human difAdipos that are not only morphologically and genotypically comparable to mAdipos, but also functionally resemble mAdipos.

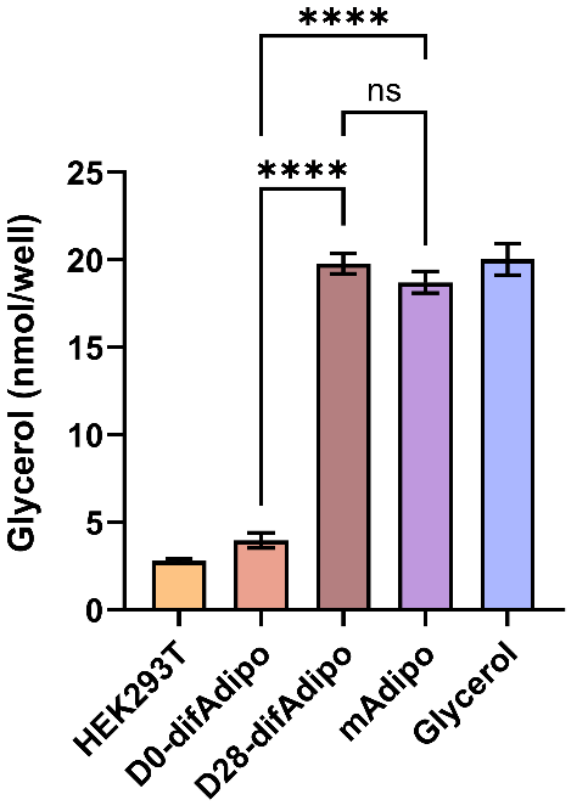

Figure 4. Differentiated adipocytes (difAdipos) exhibit lipolytic function comparable to mature adipocytes (mAdipos). Lipolytic activity was assessed in preAdipos, difAdipos, and mAdipos by stimulating cells with isoproterenol and measuring glycerol release. D0 difAdipos reflect undifferentiated adipocytes and exhibited low-level lipolytic activity similar to HEK293T cells (negative control). D28 difAdipos exhibited lipolytic activity comparable to mAdipos and glycerol (positive control), validating the differentiation protocol and confirming that difAdipos functionally resemble mature adipocytes in their lipolytic activity. Statistical analysis was performed using one-way ANOVA with Sidaks multiple comparison test. A value of $P < 0.05$ was deemed statistically significant (*< 0.05; **< 0.01; ***< 0.001; ****< 0.0001).

Multiparametric characterization of EVs from differentiated adipocytes

After validating our difAdipos as robust surrogates for mAdipos, we next sought to characterize EVs from paired preAdipos, difAdipos, and mAdipos obtained from the

230 same individual (**Figure 5A**). Microfluidic resistive pulse sensing analysis revealed a
231 relatively narrow particle size distribution among the EVs from preAdipo, difAdipo, and
232 mAdipo. Median particle diameters were similar across the three Adipo populations
233 (88.5 nm for preAdipo, 91.8 nm for difAdipo, and 85.1 nm for mAdipo). All three ADEV
234 sources had similar mean particle concentrations: 6.26E+10 particles/mL for mAdipos,
235 3.47E+10 particles/mL for preAdipos and 2.33E+10 particles/mL for difAdipos **(Figure**
236 **5A).** These results suggest that our differentiation protocol did not alter the ability of
237 difAdipos to generate small EVs that were similar in size and concentration to native
238 populations (ie. preAdipos and mAdipos), which did not undergo in vitro maturation.

239 TEM revealed a polydispersed and prominent population of small EVs with the
240 characteristic artefactual 'cup-shaped' morphology **(Figure 5B).** Immunoblotting of
241 difAdipo-EVs demonstrated a heterogeneous expression of the typical EV markers
242 CD9, CD81, and CD63 and the absence of the non-EV marker calnexin (CANX) **(Figure**
243 **5C)**. The adipocyte marker, ADIPOQ, was also detected (**Figure 5C)**. Collectively, these
244 findings highlight the diversity of tissue-derived EV populations from varied adipocyte
245 sources within the same individual and at different stages of adipocyte differentiation.

246

247

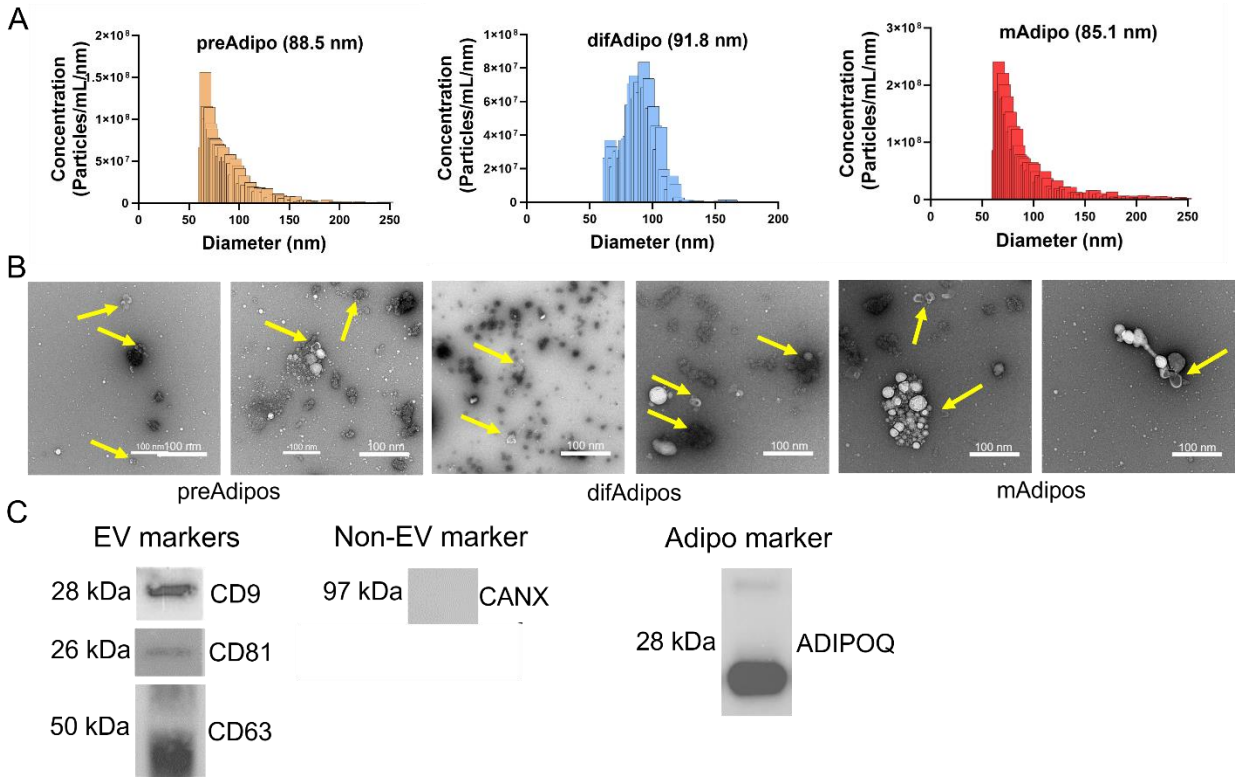

Figure 5. Multiparametric characterization of matched adipose tissue-derived EVs from the same bariatric patients. (A) MRPS analysis of EVs from preAdipo, difAdipo, and mAdipo from the same individuals (n = 3 biological replicated). Median particle diameters: 88.5 nm (preAdipo), 91.8 nm (difAdipo), 85.1 nm (mAdipo). Mean particle concentrations: 3.47E+10 particles/mL (preAdipo), 2.33E+10 particles/mL (difAdipo), 6.26E+10 particles/mL (mAdipo). (B) TEM imaging showed a polydispersed population of particles, including small EVs with a characteristic 'cup-shaped' morphology. (C) Immunoblot analysis of EVs from difAdipo reveals heterogeneous expression of typical EV (CD9, CD81, CD63), non-EV (CANX), and adipose-specific (ADIPOQ) markers. MRPS, microfluidic resistive pulse sensing; TEM, transmission electron microscopy.

High-resolution, simultaneous detection of human adipose-derived EV proteins and RNA using total internal reflection fluorescence (TIRF) microscopy

TIRF microscopy was utilized to achieve simultaneous detection of human adipose-derived EV proteins and RNA and colocalization of the same (**Figure 6 A, B).**

First, we investigated the colocalization of EV surface proteins and EV mRNA cargo in preAdipo-EVs and difAdipo-EVs to confirm the specificity of adipocyte-EVs. DifAdipo-EVs revealed high colocalization between OCT4 protein and ADIPOQ mRNA, confirming the adipocyte-specificity of the EVs. The tetraspanin marker CD63 showed less to no colocalization with other biomarkers (Figure 6A), underscoring the heterogeneous expression profile of tetraspanins. Similar results were observed for preAdipo-EVs (results not shown).

Next, we quantified the relative fluorescence intensity of EV surface markers and mRNA cargo (**Figure 6B**). DifAdipo-EVs collected on day 28, compared to preAdipo-EVs collected on day 2, expressed a significantly higher level of the canonical EV marker CD63 (***< 0.001). Interestingly, the protein marker for undifferentiated adipocytes, OCT4, was also significantly higher on difAdipo-EVs than preAdipo-EVs (*< 0.05). The expression levels of adipose tissue-specific protein and gene markers, such as adipocyte plasma membrane-associated protein (APMAP) and ADIPOQ, were similar between the difAdipo-EVs and preAdipo-EVs. In summary, APMAP and ADIPOQ exhibited stable expression levels across the maturation process, while CD63 and OCT4 were dynamically regulated during the same differentiation process.

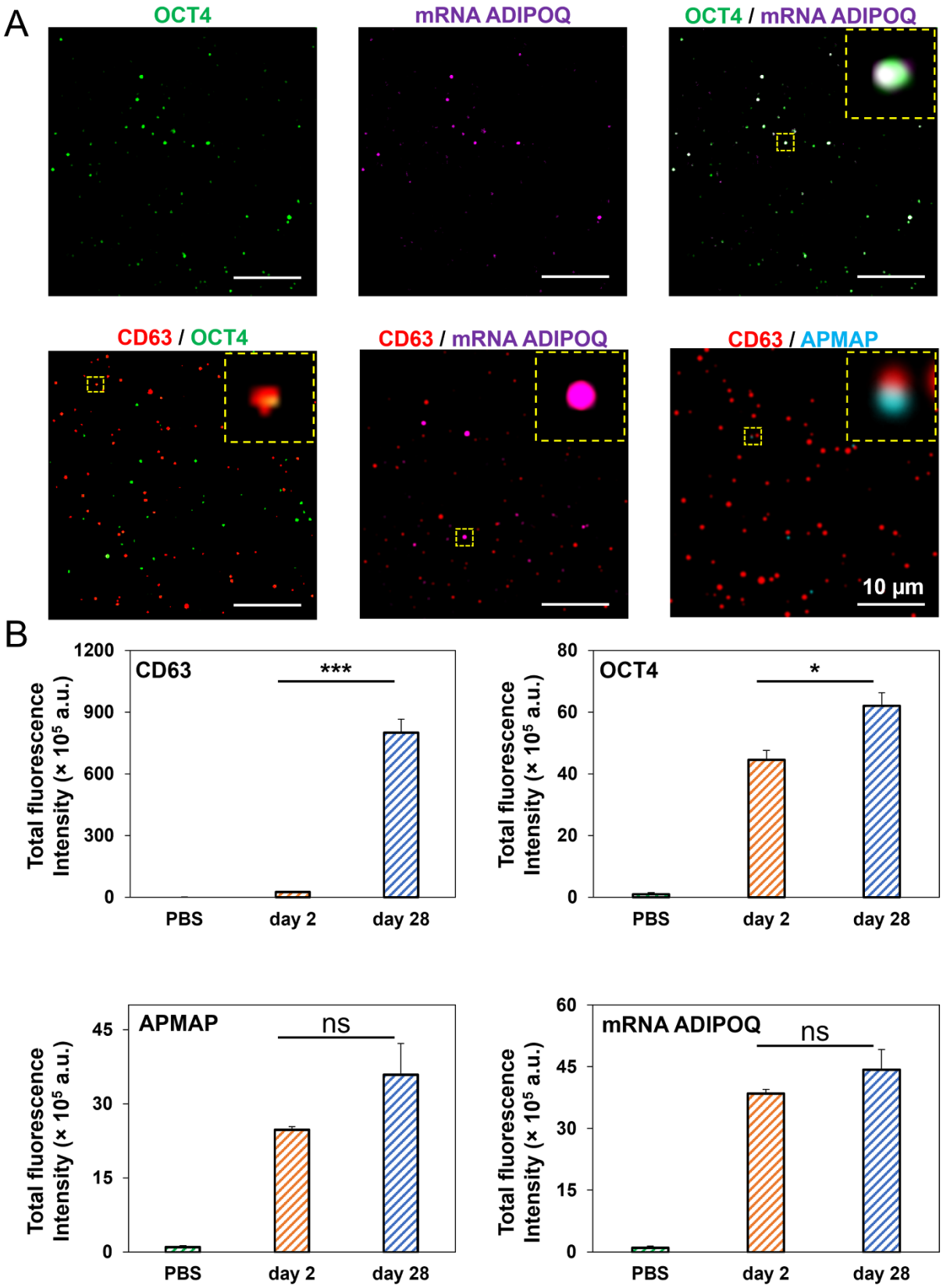
A
OCT4
mRNA ADIPOQ
OCT4 / mRNA ADIPOQ
CD63 / OCT4
CD63 / mRNA ADIPOQ
CD63 / APMAP
10 µm
B
CD63
***
Total fluorescence Intensity (× 10^5 a.u.)
1200
900
600
300
0
PBS
day 2
day 28
OCT4
*
80
60
40
20
0
APMAP
ns
45
30
15
mRNA ADIPOQ
ns

281

Figure 6. Single EV multiparametric characterization comparing preAdipo-EVs (day 2) and difAdipo-EVs (day 28). (A) Representative TIRFM images illustrating (day 28) EVs were captured by anti-CD9 and anti-CD63 antibodies and immobilized on a biochip surface. Detection antibodies against CD63, OCT, and APMAP were used to identify EV surface proteins. A fluorescence-labeled molecular beacon detected the mRNA ADIPOQ within those EVs. The merged image reveals difAdipo-EVs defined by colocalization of OCT4 and mRNA ADIPOQ, CD63 and Oct4, CD63 and mRNA ADIPOQ, CD63 and APMAP Scale 10 µm (B) The relative fluorescence intensity of EVs collected at day 2 and day 28 was analyzed for the tetraspanin marker CD63, the undifferentiated cell marker OCT4, the adipocyte plasma membrane-associated protein APMAP, and the adipose tissue gene marker mRNA ADIPOQ. OCT4, octamer-binding transcription factor 4; ADIPOQ, adiponectin; APMAP, astrocyte membrane-associated protein. Statistical analysis was performed using students test. A value of $P < 0.05$ was deemed statistically significant (*< 0.05; **< 0.01; ***< 0.001; ****< 0.0001).

Discussion

Adipose-derived EVs are increasingly recognized as critical orchestrators in obesity-associated diseases[46]. Limited studies have characterized human adipocyte EVs[47-51] , however, no study has systematically studied paired difAdipo-EVs and mAdipo-EVs at bulk and single EV resolutions. Herein, we present a reproducible and scalable surrogate source of human mature-like adipocytes (difAdipos) that exhibit phenotypic, genotypic, and functional properties paralleling those of paired mature adipocytes (mAdipos). Furthermore, we demonstrate that in vitro difAdipos can release ADEVs comparable to ADEVs released by mature adipocytes. Finally, we provide the first high-resolution, single EV analysis of human difAdipo-EVs, demonstrating simultaneous adipocyte-enriched gene transcript and surface protein markers.

Due to recognized cross-species differences[52,53] between mouse and human adipose biology, adipocyte EVs from rodent models have limited direct human translational utility. Several alternate approaches to circumvent the cross-species differences include

studying in vitro differentiated human adipocytes, adipose tissue explants, and circulating adipocyte-enriched EV subpopulations in human biofluids[54]. Kranendonk and colleagues were amongst the earliest groups to characterize human adipocyte EVs (defined as adiponectin and fatty-acid binding protein 4 positive EVs), isolated from the Human Simpson Golabi Behmel Syndrome (SGBS) cell line[55] . More recently, a study by Clement and collaborators isolated primary human adipocytes from dermolipectomy-derived subcutaneous adipose tissue and demonstrated the functional ability of isolated human adipocyte EVs to metabolically remodel melanoma cells into a more invasive phenotype[56]. Several human ADEV studies have utilized tissue explants for ADEVs rather than mature adipocytes[51,57] . Human adipose tissue explants have the advantage of overcoming the cross-species limitations of mouse models but confound the ability to investigate the potential pathobiological role of EVs shed solely from mature adipocytes[58]which are the most abundant and primary functional metabolic cells within visceral adipose tissue[49,59].

A less invasive and more feasible approach for studying human ADEVs involves interrogating the circulating pool of all EVs and attempting to enrich for EV subpopulations that contain ‘adipocyte-specific’ markers. Connolly and colleagues were the first to confirm human EVs containing adipose-enriched markers within the circulating pool of plasma-derived EVs from obese individuals[60] . In this study, the authors applied contemporaneous ISEV guidelines[61] for EV research and used complementary EV isolation and enrichment methods to attempt to account for non-vesicular co-isolates and non-adipose EV populations.

One of the formidable challenges in studying cell and tissue-specific EVs, such as ADEVs, arises from their low abundance and high signal-to-noise ratio[58,62] . Adipose EVs are estimated to comprise >80% of tissue-derived EVs in human plasma and can be the primary source of circulating miRNAs; however, tissue-derived EVs comprise <0.2 % of the circulating human plasma pool [63-65]. This limitation underscores the critical need for more advanced methods to study low-abundant, rare EV subpopulations. To address this limitation, we first produced a surrogate source of functional mature adipocytes in vitro and demonstrated their ability to shed EVs

comparable in adipocyte-specific markers to EVs shed by adipocytes that matured in vivo.

To our knowledge, no studies have characterized the biophysical properties of human adipose-derived EVs in the pre- and post-adipogenic phases from paired human biospecimens. One study conducted a systematic phenotypic comparison between immature and mature mouse ADEVs[66]. In this study, the authors characterized the biophysical properties of pre- and post-adipogenic adipocyte-derived EVs from 3T3-L1 cells. Similar to the Connolly study, we found the highest expression of the preAdipo marker PREF-1 in the earliest stages of differentiation and the highest expression of the mAdipo marker ADIPOQ in the later stages of maturation. They also found increased secretion of small EVs in the early stages of differentiation, slightly increased CD9 and CD63 protein via time-resolved fluorescence, and a higher proportion of phospholipids associated with cell signaling. Interestingly, the authors found EV-unique characteristics that differed from the 3T3-L1 parental cell, suggesting modifications that could impact EV-mediated intercellular communication[66].

Finally, we applied single EV multiplexing analytics to validate the adipocyte-specificity of our difAdipo-EVs. Colocalization of EV surface proteins and internal cargo can increase sensitivity for detecting low-abundance EV subpopulations and can also enhance the biomarker utility of EVs to detect earlier stages of disease[70,71] . Therefore, our single ADEV multiplexing platform holds great promise for investigating novel and robust, adipocyte-specific EVs in obesity-associated diseases.

Conclusion

Our study presents a novel paradigm for advancing the translational application of human ADEVs by using human difAdipos as a surrogate for mature adipocytes, thereby augmenting the harvesting of viable human-derived, mature adipocyte EVs. The model established provides a high-yield, functionally equivalent source of EVs, facilitating more consistent and relevant research into the role of ADEVs in obesity and metabolic diseases. Our findings underscore the importance of adipocyte differentiation on EV

content and function, revealing significant differences in biomarker profiles between preAdipo-EVs and difAdipo-EVs. This differentiation may impact the bioactive cargo within the EVs, influencing recipient cell behavior and contributing to metabolic complications associated with obesity.

Future research should explore the specific mechanisms by which difAdipo-EVs influence metabolic processes and their potential as biomarkers or therapeutic targets in obesity-related conditions. This study herein lays the groundwork for developing therapeutic strategies that modulate ADEVs' effects, offering promising avenues for mitigating the adverse consequences of obesity on metabolic health and reducing the risk of associated diseases.

Materials and methods

Study participants

This study complies with all relevant ethical guidelines. The Ohio State University Institutional Review Board (IRB# 2014H0471) approved the study, and all participants provided written informed consent. Visceral adipose tissue (VAT) samples were collected from patients (n = 11, mean age: 41.6 years, SD: 12.98; mean BMI: 40.97, SD: 6.00) undergoing elective bariatric surgery at The Ohio State University (OSU) Center for Minimally Invasive Surgery. Clinical data are summarized in Table S1.

Adipose tissue dissociation and mature adipocyte culture for EV isolation

Adipose tissue samples were collected in the operating room during the bariatric surgery and processed within 1 hr using collagenase digestion, as previously described [25]. The cell suspension was centrifuged at 500 x g for 10 min to generate three distinct phases (mature adipocytes, the stromal vascular fraction (SVF), and the SVF secretome). Floating mature adipocytes were carefully removed from the top layer and kept for culture. The supernatant was then carefully aspirated to avoid disturbing the SVF pellet, which was resuspended in sorting media for the pre-adipocyte isolation and differentiation protocol (see below). Mature adipocytes were cultured for 24 hr in Dulbecco's Modified Eagle Medium/Ham's Nutrient Mixture F-12 (DMEM/F12),

397 supplemented with 40% M199 basal medium with Earle's salts and L-glutamine
398 (MCDB201), 2% fetal bovine serum (FBS), 1x penicillin/streptomycin, 1 nM
399 dexamethasone, 0.1 mM L-ascorbic acid 2-phosphate (LAAP), 1x Insulin-Transferrin-
400 Selenium (ITS) Mix, 1x linoleic acid-albumin, 5 μg/μL insulin, and 1 nM triiodothyronine
401 (T3).

402 **Preadipocyte (preAdipo) isolation and differentiation into differentiated mature**
403 **adipocytes (difAdipos)**
404
405 The resuspended SVF pellet was filtered through a 100 μm cell strainer into fresh tubes,
406 repeating the washing step to ensure thorough isolation of SVF cells. Following another
407 round of centrifugation (at 1200 rpm for 10 min at RT or 4 °C), and aspiration of the
408 supernatant, the SVF pellet was treated with ACK lysis buffer on ice for three minutes to
409 lyse any remaining red blood cells, followed by dilution and filtration through a 40 μm
410 cell strainer. Finally, the SVF pellet containing cells were re-suspended in sorting media
411 and seeded into culture plates until the cells reached approximately 80% confluency.
412 The differentiation process commenced with a 24 hr incubation in growth media,
413 designated as day 0. Throughout the differentiation period, media was replaced every
414 48 hr. Cells were maintained for up to 28 days in adipogenic induction media 1 and 2
415 (AIM1 and AIM 2). For media composition, see Table S3.

416 **ADEV isolation via tangential flow filtration (TFF)**

417 PreAdipo, difAdipo and mAdipo culture media was filtered through 0.2 μm filters and
418 then concentrated to 5 mL. The concentrated media was diafiltered using TFF with a
419 500 kDa filter for purification at a flow rate of 35 mL/min, as previously described [25].
420 Following TFF, the retentates were further concentrated using centrifugal units (30 kDa
421 MWCO, MilliporeSigma Amicon Ultra Centrifugal Filter Unit, Fisher Scientific) at 4000 ×
422 g for 30 min to a final volume of 100 μL.

423 **Microfluidic resistive pulse sensing (MRPS)**

424 Particle concentration and size distribution were measured using microfluidic resistive
425 pulse sensing with the Spectradyne nCS1 instrument (Spectradyne, Torrance, CA),

426 equipped with C-400 polydimethylsiloxane cartridges to cover a size range of
427 approximately 65-400 nm [25]. Data analysis was performed using the nCS1 Data
428 Analyzer (Spectradyne, Torrance, CA).

429 **Western blotting**

430 EV samples were lysed in radioimmunoprecipitation assay (RIPA) buffer (Thermo
431 Scientific) and treated with protease and phosphatase inhibitor (Thermo Scientific) for
432 15 min on ice. Protein concentration was quantified using a Micro BCA™ Protein Assay
433 Kit (Thermo Scientific). Equivalent amounts of protein in Laemmli buffer (with reducing
434 agent 2-mercaptoethanol, Sigma-Aldrich) were electrophoresed on 4-20% Mini-
435 PROTEAN® TGX Stain-Free gels (Bio-Rad) and then transferred onto a polyvinylidene
436 fluoride (PVDF) membrane (Bio-Rad). Membranes were blocked and then probed with
437 primary antibody diluted in TBS-T overnight at 4 °C, followed by incubation with
438 horseradish peroxidase-conjugated secondary antibody for 1 hr at room temperature.
439 Immunoreactivity was detected using enhanced chemiluminescence (ECL) solutions
440 (Bio-Rad) and visualized using a Bio-Rad ChemiDoc™ MP imaging system.

441 **Quantification of real-time polymerase chain reaction (qRT-PCR)**

442 Total RNA was isolated using the RNeasy Mini Kit (Qiagen) according to the
443 manufacturer's instructions and quantified using a NanoDrop spectrophotometer. The
444 isolated RNA was reverse-transcribed into cDNA using the High-Capacity cDNA
445 Reverse Transcription Kit (Applied Biosystems). Real-time PCR was performed with the
446 PowerUp™ SYBR™ Green Master Mix (Thermo Fisher) on an Applied Biosystems real-
447 time PCR system. The sequences of the forward and reverse primers are listed in Table
448 S4. β-actin was used as the internal normalization control.

449 **Lipolysis assay**

450 To investigate mature adipocyte functional activity, a lipolysis assay was performed
451 using the Lipolysis Assay Kit (Abcam) per the manufacturer's instructions. Day 0
452 (preAdipo), day 28 (difAdipo), and cultured HEK293 (negative control) cells were
453 washed twice with Lipolysis Wash Buffer, then stimulated with 100 nM isoproterenol for

454 4 hr. Absorbance at 570 nm was measured using the SpectraMax iD3 (Molecular
455 Devices), and glycerol concentration was quantified using a standard curve.

456 **Transmission electron microscopy (TEM)**

457 TEM was performed as previously described[26]. Briefly, TEM grids were first treated with
458 plasma for high surface EVs absorption. Subsequently, 10 μL of EVs samples were
459 drop-casted onto the plasma-treated surface. The samples were incubated for 1 minute
460 and then blotted with filter paper to remove excess liquid. The TEM grids were washed
461 twice in DI water and stained with UranyLess EM contrast stain (Electron Microscopy
462 Science) for 22 sec. The TEM grids were dried overnight prior to imaging. TEM images
463 were obtained using Tecnai TF-20 microscope under 200kV, bright-field imaging mode.

464 **Single EV analysis using total internal reflection fluorescence microscopy (TIRF)**

465 The isolated EVs were captured and analyzed on a gold functionalized biochip following
466 our previous protocol [25]. Briefly, the EVs collected on day 2 (preAdipo-EVs) and day 28
467 (difAdipo-EVs) were permeabilized and hybridized with molecular beacons (Table S5) in
468 0.5 × Tris EDTA (TE) buffer at 0.2 μM concentration for 2 hr at 37 °C in a dark
469 environment to facilitate molecular beacon hybridization to the target RNA. The EV
470 samples were incubated on the biochip surface and captured by functionalized anti-
471 CD63 and anti-CD9 antibodies. Proteins were detected using fluorescent-dye-
472 conjugated antibodies. Finally, a 10 × 10 array of images was acquired via total internal
473 reflection fluorescence microscope (TIRFM; Nikon, Melville, NY) for each well. Relative
474 and total fluorescence intensities of the sample were obtained from custom-built
475 algorithms that were previously reported [27,28]
476

477 **Data availability**

478 All data generated or analyzed during this study are included in this manuscript and its
479 supplementary information file. Further inquiries can be directed to the corresponding
480 author.
481

482 **Author contributions**

483 Conceptualization: BLB., M.D.H., P.L.P., W.H., E.R., S.M.M,

Study design and funding acquisition: E.R., S.M.M.

Investigation and performed research: M.D.H., B.L.B., P.L.P., D.S., K.T.N., S.N., S.A.B., B.J.N.

Organization and data analysis: M.D.H., B.L.B, K.T.N

Completed the original draft of the manuscript: M.D.H., B.L.B., S.M.M

Data interpretation, revision, and manuscript correction: M.D.H., B.L.B., K.T.N., E.R., S.M.M.

All authors approved the final version of the manuscript.

Competing interests

The authors declare no competing interests.

Additional information

Correspondence and requests for materials should be addressed to Senior Corresponding author.

Acknowledgments

We would like to thank William Ray for his illustrative media expertise in designing the figures for this project. SMM was supported by intramural funding from the Abigail Wexner Research Institute at Nationwide Children's Hospital and NINDS (5K12NS098482-05). ER was supported by National Institutes of Health (NIH) grants UG3/UH3TR002884 and U18TR003807. The content is solely the responsibility of the authors and does not necessarily represent the official views of the National Institutes of Health.

References

1 Blüher, M. Obesity: global epidemiology and pathogenesis. *Nature Reviews Endocrinology* **15**, 288-298 (2019). https://doi.org:10.1038/s41574-019-0176-8

2 Seidell, J. C. & Halberstadt, J. The global burden of obesity and the challenges of prevention. *Ann Nutr Metab* **66 Suppl 2**, 7-12 (2015). https://doi.org:10.1159/000375143

3 Chong, B. *et al.* Trends and predictions of malnutrition and obesity in 204 countries and territories: an analysis of the Global Burden of Disease Study 2019. *eClinicalMedicine* **57**, 101850 (2023). https://doi.org:https://doi.org/10.1016/j.eclinm.2023.101850

4 Powell-Wiley, T. M. *et al.* Obesity and Cardiovascular Disease: A Scientific Statement From the American Heart Association. *Circulation* **143**, e984-e1010 (2021). https://doi.org:10.1161/CIR.0000000000000973

5 Avgerinos, K. I., Spyrou, N., Mantzoros, C. S. & Dalamaga, M. Obesity and cancer risk: Emerging biological mechanisms and perspectives. *Metabolism* **92**, 121-135 (2019). https://doi.org:10.1016/j.metabol.2018.11.001

6 Sarwar, R., Pierce, N. & Koppe, S. Obesity and nonalcoholic fatty liver disease: current perspectives. *Diabetes Metab Syndr Obes* **11**, 533-542 (2018). https://doi.org:10.2147/dmso.S146339

7 Picone, P., Di Carlo, M. & Nuzzo, D. Obesity and Alzheimer's disease: Molecular bases. *Eur J Neurosci* **52**, 3944-3950 (2020). https://doi.org:10.1111/ejn.14758

8 Shaikh, S. R., Beck, M. A., Alwarawrah, Y. & MacIver, N. J. Emerging mechanisms of obesity-associated immune dysfunction. *Nature Reviews Endocrinology* **20**, 136-148 (2024). https://doi.org:10.1038/s41574-023-00932-2

9 Kawai, T., Autieri, M. V. & Scalia, R. Adipose tissue inflammation and metabolic dysfunction in obesity. *Am J Physiol Cell Physiol* **320**, C375-c391 (2021). https://doi.org:10.1152/ajpcell.00379.2020

10 Kershaw, E. E. & Flier, J. S. Adipose tissue as an endocrine organ. *J Clin Endocrinol Metab* **89**, 2548-2556 (2004). https://doi.org:10.1210/jc.2004-0395

11 Booth, A., Magnuson, A., Fouts, J. & Foster, M. T. Adipose tissue: an endocrine organ playing a role in metabolic regulation. *Horm Mol Biol Clin Investig* **26**, 25-42 (2016). https://doi.org:10.1515/hmbci-2015-0073

12 Ouchi, N., Parker, J. L., Lugus, J. J. & Walsh, K. Adipokines in inflammation and metabolic disease. *Nature Reviews Immunology* **11**, 85-97 (2011). https://doi.org:10.1038/nri2921

13 Longo, M. *et al.* Adipose Tissue Dysfunction as Determinant of Obesity-Associated Metabolic Complications. *Int J Mol Sci* **20** (2019). https://doi.org:10.3390/ijms20092358

14 Kalluri, R. & LeBleu, V. S. The biology, function, and biomedical applications of exosomes. *Science* **367** (2020). https://doi.org:10.1126/science.aau6977

15 Hade, M. D., Suire, C. N. & Suo, Z. Mesenchymal Stem Cell-Derived Exosomes: Applications in Regenerative Medicine. *Cells* **10**, 1959 (2021).

16 Tkach, M. & Thery, C. Communication by Extracellular Vesicles: Where We Are and Where We Need to Go. *Cell* **164**, 1226-1232 (2016). https://doi.org:10.1016/j.cell.2016.01.043

17 Connolly, K. D., Rees, D. A. & James, P. E. Role of adipocyte-derived extracellular vesicles in vascular inflammation. *Free Radic Biol Med* **172**, 58-64 (2021). https://doi.org:10.1016/j.freeradbiomed.2021.04.031

18 Isaac, R., Reis, F. C. G., Ying, W. & Olefsky, J. M. Exosomes as mediators of intercellular crosstalk in metabolism. *Cell Metab* **33**, 1744-1762 (2021). https://doi.org:10.1016/j.cmet.2021.08.006

19 Zhou, C., Huang, Y.-Q., Da, M.-X., Jin, W.-L. & Zhou, F.-H. Adipocyte-derived extracellular vesicles: bridging the communications between obesity and tumor microenvironment. *Discover Oncology* **14**, 92 (2023). https://doi.org:10.1007/s12672-023-00704-4

20 Kumar, V., Kiran, S., Kumar, S. & Singh, U. P. Extracellular vesicles in obesity and its associated inflammation. *Int Rev Immunol* **41**, 30-44 (2022). https://doi.org:10.1080/08830185.2021.1964497

21 Crewe, C. The challenges of interrogating adipose tissue extracellular vesicle functions in physiology. *Commun Biol* **5**, 581 (2022). https://doi.org:10.1038/s42003-022-03511-9

22 Crewe, C. *et al.* An Endothelial-to-Adipocyte Extracellular Vesicle Axis Governed by Metabolic State. *Cell* **175**, 695-708 e613 (2018). https://doi.org:10.1016/j.cell.2018.09.005

23 Akbar, N., Pinnick, K. E., Paget, D. & Choudhury, R. P. Isolation and Characterization of Human Adipocyte-Derived Extracellular Vesicles using Filtration and Ultracentrifugation. *J Vis Exp* (2021). https://doi.org:10.3791/61979

24 Borgeson, E., Boucher, J. & Hagberg, C. E. Of mice and men: Pinpointing species differences in adipose tissue biology. *Front Cell Dev Biol* **10**, 1003118 (2022). https://doi.org:10.3389/fcell.2022.1003118

25 Palacio, P. L. *et al.* Novel multiparametric bulk and single EV pipeline for adipose cell-specific biomarker discovery in paired human biospecimens. *bioRxiv*, 2024.2004.2018.590172 (2024). https://doi.org:10.1101/2024.04.18.590172

26 Nguyen, K. T. *et al.* Integrated Techniques for Extracellular Particle Separation and Single-Particle Multiparametric Characterization to Track Cancer Biomarkers from Tissue to Biofluids. *bioRxiv*, 2025.2001.2009.632270 (2025). https://doi.org:10.1101/2025.01.09.632270

27 Rima, X. Y. *et al.* Microfluidic harvesting of breast cancer tumor spheroid-derived extracellular vesicles from immobilized microgels for single-vesicle analysis. *Lab Chip* **22**, 2502-2518 (2022). https://doi.org:10.1039/d1lc01053k

28 Nguyen, L. T. H. *et al.* An immunogold single extracellular vesicular RNA and protein ((Au) SERP) biochip to predict responses to immunotherapy in non-small cell lung cancer patients. *J Extracell Vesicles* **11**, e12258 (2022). https://doi.org:10.1002/jev2.12258

29 Vella, L. J. *et al.* A rigorous method to enrich for exosomes from brain tissue. *J Extracell Vesicles* **6**, 1348885 (2017). https://doi.org:10.1080/20013078.2017.1348885

30 Tong, Q. *et al.* Function of GATA Transcription Factors in Preadipocyte-Adipocyte Transition. *Science* **290**, 134-138 (2000). https://doi.org:doi:10.1126/science.290.5489.134

31 da Silva, C., Durandt, C., Kallmeyer, K., Ambele, M. A. & Pepper, M. S. The Role of Pref-1 during Adipogenic Differentiation: An Overview of Suggested Mechanisms. *Int J Mol Sci* **21** (2020). https://doi.org:10.3390/ijms21114104

32 Tseng, Y.-H. *et al.* Prediction of preadipocyte differentiation by gene expression reveals role of insulin receptor substrates and necdin. *Nature Cell Biology* **7**, 601-611 (2005). https://doi.org:10.1038/ncb1259

33 Rim, J. S. *et al.* Direct Conversion of Human Preadipocytes into Hematopoietic, Neuronal, and Pancreatic α Cells by Oct4 and Klf4 Overexpression. *BioResearch Open Access* **4**, 389-397 (2015). https://doi.org:10.1089/biores.2015.0028

34 Dang, T. N. *et al.* Expression of the preadipocyte marker ZFP423 is dysregulated between well-differentiated and dedifferentiated liposarcoma. *BMC Cancer* **22**, 300 (2022). https://doi.org:10.1186/s12885-022-09379-6

35 Noguchi, Y., Murakami, M., Murata, M. & Kano, F. Microscopic image-based classification of adipocyte differentiation by machine learning. *Histochemistry and Cell Biology* **159**, 313-327 (2023). https://doi.org:10.1007/s00418-022-02168-z

36 Audano, M. *et al.* Regulatory mechanisms of the early phase of white adipocyte differentiation: an overview. *Cellular and Molecular Life Sciences* **79**, 139 (2022). https://doi.org:10.1007/s00018-022-04169-6

37 Tong, Q. *et al.* Function of GATA transcription factors in preadipocyte-adipocyte transition. *Science* **290**, 134-138 (2000). https://doi.org:10.1126/science.290.5489.134

38 Al-Mansoori, L. *et al.* Suppression of GATA-3 increases adipogenesis, reduces inflammation and improves insulin sensitivity in 3T3L-1 preadipocytes. *Cellular Signalling* **75**, 109735 (2020). https://doi.org:https://doi.org/10.1016/j.cellsig.2020.109735

39 Fu, Y., Luo, N., Klein, R. L. & Garvey, W. T. Adiponectin promotes adipocyte differentiation, insulin sensitivity, and lipid accumulation. *Journal of Lipid Research* **46**, 1369-1379 (2005). https://doi.org:https://doi.org/10.1194/jlr.M400373-JLR200

40 Itabe, H., Yamaguchi, T., Nimura, S. & Sasabe, N. Perilipins: a diversity of intracellular lipid droplet proteins. *Lipids in Health and Disease* **16**, 83 (2017). https://doi.org:10.1186/s12944-017-0473-y

41 Sztalryd, C. & Brasaemle, D. L. The perilipin family of lipid droplet proteins: Gatekeepers of intracellular lipolysis. *Biochim Biophys Acta Mol Cell Biol Lipids* **1862**, 1221-1232 (2017). https://doi.org:10.1016/j.bbalip.2017.07.009

42 Daya, S., Loughlin, A. J. & MacQueen, H. A. Culture and differentiation of preadipocytes in two-dimensional and three-dimensional in vitro systems. *Differentiation* **75**, 360-370 (2007). https://doi.org:https://doi.org/10.1111/j.1432-0436.2006.00146.x

43 Nielsen, T. S., Jessen, N., Jørgensen, J. O. L., Møller, N. & Lund, S. Dissecting adipose tissue lipolysis: molecular regulation and implications for metabolic disease. *Journal of Molecular Endocrinology* **52**, R199-R222 (2014). https://doi.org:10.1530/jme-13-0277

44 Yang, A. & Mottillo, E. P. Adipocyte lipolysis: from molecular mechanisms of regulation to disease and therapeutics. *Biochem J* **477**, 985-1008 (2020). https://doi.org:10.1042/bcj20190468

45 Cho, C. H., Patel, S. & Rajbhandari, P. Adipose tissue lipid metabolism: lipolysis. *Current Opinion in Genetics & Development* **83**, 102114 (2023). https://doi.org:https://doi.org/10.1016/j.gde.2023.102114

46 Crewe, C. & Scherer, P. E. Intercellular and interorgan crosstalk through adipocyte extracellular vesicles. *Rev Endocr Metab Disord* **23**, 61-69 (2022). https://doi.org:10.1007/s11154-020-09625-x

47 Kranendonk, M. E. *et al.* Human adipocyte extracellular vesicles in reciprocal signaling between adipocytes and macrophages. *Obesity (Silver Spring)* **22**, 1296-1308 (2014). https://doi.org:10.1002/oby.20679

48 Lazar, I. *et al.* Adipocyte Exosomes Promote Melanoma Aggressiveness through Fatty Acid Oxidation: A Novel Mechanism Linking Obesity and Cancer. *Cancer Research* **76**, 4051-4057 (2016). https://doi.org:10.1158/0008-5472.CAN-16-0651

49 Clement, E. *et al.* Adipocyte extracellular vesicles carry enzymes and fatty acids that stimulate mitochondrial metabolism and remodeling in tumor cells. *Embo j* **39**, e102525 (2020). https://doi.org:10.15252/embj.2019102525

50 Matilainen, J. *et al.* Increased secretion of adipocyte-derived extracellular vesicles is associated with adipose tissue inflammation and the mobilization of excess lipid in human obesity. *J Transl Med* **22**, 623 (2024). https://doi.org:10.1186/s12967-024-05249-w

51 Kulaj, K. *et al.* Adipocyte-derived extracellular vesicles increase insulin secretion through transport of insulinotropic protein cargo. *Nat Commun* **14**, 709 (2023). https://doi.org:10.1038/s41467-023-36148-1

52 Börgeson, E., Boucher, J. & Hagberg, C. E. Of mice and men: Pinpointing species differences in adipose tissue biology. *Front Cell Dev Biol* **10**, 1003118 (2022). https://doi.org:10.3389/fcell.2022.1003118

53 Muniyappa, R. *et al.* Comparison between surrogate indexes of insulin sensitivity/resistance and hyperinsulinemic euglycemic clamp estimates in rats. *Am J Physiol Endocrinol Metab* **297**, E1023-1029 (2009). https://doi.org:10.1152/ajpendo.00397.2009

54 Gómez-Serrano, M., Ponath, V., Preußer, C. & Pogge von Strandmann, E. Beyond the Extracellular Vesicles: Technical Hurdles, Achieved Goals and Current Challenges When Working on Adipose Cells. *Int J Mol Sci* **22** (2021). https://doi.org:10.3390/ijms22073362

55 Kranendonk, M. E. G. *et al.* Human adipocyte extracellular vesicles in reciprocal signaling between adipocytes and macrophages. *Obesity* **22**, 1296-1308 (2014). https://doi.org:https://doi.org/10.1002/oby.20679

56 Sarango, G. *et al.* The Autophagy Receptor TAX1BP1 (T6BP) improves antigen presentation by MHC-II molecules. *EMBO Rep* **23**, e55470 (2022). https://doi.org:10.15252/embr.202255470

57 Chatterjee, E. *et al.* The extracellular vesicle transcriptome provides tissue-specific functional genomic annotation relevant to disease susceptibility in obesity. *medRxiv* (2024). https://doi.org:10.1101/2024.11.18.24317277

58 Gómez-Serrano, M., Ponath, V., Preußer, C. & Pogge von Strandmann, E. Beyond the Extracellular Vesicles: Technical Hurdles, Achieved Goals and Current Challenges When Working on Adipose Cells. *International Journal of Molecular Sciences* **22**, 3362 (2021).

59 Sethi, J. K. & Vidal-Puig, A. J. Thematic review series: Adipocyte Biology. Adipose tissue function and plasticity orchestrate nutritional adaptation. *Journal of Lipid Research* **48**, 1253-1262 (2007). https://doi.org:https://doi.org/10.1194/jlr.R700005-JLR200

60 Connolly, K. D. *et al.* Evidence for Adipocyte-Derived Extracellular Vesicles in the Human Circulation. *Endocrinology* **159**, 3259-3267 (2018). https://doi.org:10.1210/en.2018-00266

61 Lötvall, J. *et al.* Minimal experimental requirements for definition of extracellular vesicles and their functions: a position statement from the International Society for Extracellular Vesicles. *J Extracell Vesicles* **3**, 26913 (2014). https://doi.org:10.3402/jev.v3.26913

62 Adnan, S.-s., Benjamin, G. T. & David, R. W. Advances in extracellular vesicle isolation methods: a path towards cell-type specific EV isolation. *Extracellular Vesicles and Circulating Nucleic Acids* **4**, 447-460 (2023). https://doi.org:10.20517/evcna.2023.14

63 Beck, B. R., Shin, B., Choi, Y., Park, S. & Kang, K. Predicting commercially available antiviral drugs that may act on the novel coronavirus (SARS-CoV-2) through a drug-target interaction deep learning model. *Comput Struct Biotechnol J* **18**, 784-790 (2020). https://doi.org:10.1016/j.csbj.2020.03.025

64 Thomou, T. *et al.* Adipose-derived circulating miRNAs regulate gene expression in other tissues. *Nature* **542**, 450-455 (2017). https://doi.org:10.1038/nature21365

65 Li, Y. *et al.* EV-origin: Enumerating the tissue-cellular origin of circulating extracellular vesicles using exLR profile. *Computational and Structural Biotechnology Journal* **18**, 2851-2859 (2020). https://doi.org:https://doi.org/10.1016/j.csbj.2020.10.002

66 Connolly, K. D. *et al.* Characterisation of adipocyte-derived extracellular vesicles released pre- and post-adipogenesis. *J Extracell Vesicles* **4**, 29159 (2015). https://doi.org:10.3402/jev.v4.29159

67 Liangsupree, T., Multia, E. & Riekkola, M.-L. Modern isolation and separation techniques for extracellular vesicles. *Journal of Chromatography A* **1636**, 461773 (2021). https://doi.org:https://doi.org/10.1016/j.chroma.2020.461773

68 Ter-Ovanesyan, D. *et al.* Framework for rapid comparison of extracellular vesicle isolation methods. *Elife* **10** (2021). https://doi.org:10.7554/eLife.70725

69 Di, K. *et al.* Highly efficient and automated isolation technology for extracellular vesicles microRNA. *Front Bioeng Biotechnol* **10**, 948757 (2022). https://doi.org:10.3389/fbioe.2022.948757

70 Ferguson, S. *et al.* Single-EV analysis (sEVA) of mutated proteins allows detection of stage 1 pancreatic cancer. *Sci Adv* **8**, eabm3453 (2022). https://doi.org:10.1126/sciadv.abm3453

71 Li, Z. *et al.* Colocalization of protein and microRNA markers reveals unique extracellular vesicle subpopulations for early cancer detection. *Sci Adv* **10**, eadh8689 (2024). https://doi.org:10.1126/sciadv.adh8689